ANTIOXIDANTS & REDOX SIGNALING
Volume 16, Number 11, 2012

DOI: 10.1089/ars.2011.4210

ORIGINAL RESEARCH COMMUNICATION

Redox Control of 20S Proteasome Gating

Gustavo M. Silva,[1,2] Luis E.S. Netto,[2] Vanessa Simões,[1] Luiz F.A. Santos,[3] Fabio C. Gozzo,[3] Marcos A.A. Demasi,[4] Cristiano L.P. Oliveira,[5] Renata N. Bicev,[5] Clécio F. Klitzke,[6] Mari C. Sogayar,[4] and Marilene Demasi[1]

Abstract

The proteasome is the primary contributor in intracellular proteolysis. Oxidized or unstructured proteins can be degraded via a ubiquitin- and ATP-independent process by the free 20S proteasome (20SPT). The mechanism by which these proteins enter the catalytic chamber is not understood thus far, although the 20SPT gating conformation is considered to be an important barrier to allowing proteins free entrance. We have previously shown that S-glutathiolation of the 20SPT is a post-translational modification affecting the proteasomal activities. ***Aims:*** The goal of this work was to investigate the mechanism that regulates 20SPT activity, which includes the identification of the Cys residues prone to S-glutathiolation. ***Results:*** Modulation of 20SPT activity by proteasome gating is at least partially due to the S-glutathiolation of specific Cys residues. The gate was open when the 20SPT was S-glutathiolated, whereas following treatment with high concentrations of dithiothreitol, the gate was closed. S-glutathiolated 20SPT was more effective at degrading both oxidized and partially unfolded proteins than its reduced form. Only 2 out of 28 Cys were observed to be S-glutathiolated in the proteasomal α5 subunit of yeast cells grown to the stationary phase in glucose-containing medium. ***Innovation:*** We demonstrate a redox post-translational regulatory mechanism controlling 20SPT activity. ***Conclusion:*** S-glutathiolation is a post-translational modification that triggers gate opening and thereby activates the proteolytic activities of free 20SPT. This process appears to be an important regulatory mechanism to intensify the removal of oxidized or unstructured proteins in stressful situations by a process independent of ubiquitination and ATP consumption. *Antioxid. Redox Signal.* 16, 1183–1194.

Introduction

The 26S proteasomal complex is responsible for the degradation of ubiquitin-tagged proteins in eukaryotic cells (10, 26). Although only the 20S proteasome core (20SPT) capped with the 19S regulatory particle (namely the 26S proteasome) is able to recognize ubiquitylated substrates, 20% to 30% of the total proteasome in mammalian and yeast cells lack regulatory particles (2, 48). Alternatively, free 20SPT operates in a ubiquitin- and ATP-independent manner to degrade unstructured substrates, including oxidized proteins (1, 25, 45). Recent work indicated that the 20SPT can cleave >20% of intracellular proteins, initiating the polypeptide processing in disordered regions, including internal domains (5, 33).

Because few repair systems for protein damage are known (*e.g.*, methionine sulfoxide reductase), it is widely accepted that proteolysis is the cellular protective mechanism against

Innovation

The 20SPT is responsible for the degradation of oxidized and unstructured proteins. In the present work, we show that 20SPT S-glutathiolation increases the degradation of oxidatively modified proteins by promoting gate opening. 20SPT S-glutathiolation would take place via the oxidation of Cys residues to sulfenic acid species followed by glutathiolation. Thus, a more oxidative environment would be responsible for both an increased protein oxidation and a modification of the redox status of the proteasome contributing to the removal of oxidized proteins before their aggregation without ATP consumption because the mechanism proposed precludes the protein ubiquitylation process. The present results show an important mechanism for coping with stressful conditions to avoid protein aggregation.

[1]Laboratório de Bioquímica e Biofísica, Instituto Butantan, São Paulo, Brasil.
[2]Departamento de Genética e Biologia Evolutiva, Instituto de Biociências, Universidade de São Paulo, Brasil.
[3]Instituto de Química, Universidade Estadual de Campinas, Brasil.
[4]Departamento de Bioquímica, Instituto de Química, Universidade de São Paulo, Brasil.
[5]Instituto de Física, Universidade de São Paulo, Brasil.
[6]Laboratório Especial de Toxinologia Aplicada, Instituto Butantan, Brasil.

metabolic protein damage, and the 20SPT is the preferential protease responsible for the removal of such proteins (24). Although it is still under discussion, convincing evidence has suggested that oxidized proteins are degraded in a ubiquitin-independent manner (1, 25, 45). The mechanism by which oxidized proteins enter the 20SPT catalytic channel is not currently understood. Both higher hydrophobicity and loss of secondary structure were investigated and appear to underlie the process (5, 19, 39). Notably, many components of the ubiquitin-proteasome system are highly sensitive to oxidative stress, implying an inhibition of protein ubiquitylation (12, 30) or an uncoupling of the 26S complex (24, 52). Although the autophagy-lysosome system can play an important role in the prevention of protein aggregation (11), no convincing data have yet revealed its role in the removal of mildly oxidized proteins. Altogether, the knowledge accumulated to date is in agreement with the hypothesis that the 20SPT is able to remove oxidized proteins.

Because the 20SPT lacks regulatory units, it is unclear how its proteolytic activity is regulated. Most likely, gating regulation and substrate interaction with the 20S core particle would underlie the entrance of substrates into the 20SPT. However, the mechanisms that regulate the gating of the free 20SPT pool are still elusive. Furthermore, there has been no systematic study of the conformational state of the free 20SPT pool in any cellular model. The 20SPT is composed of four heptameric rings ($\alpha_7\beta_7\beta_7\alpha_7$) arranged in a barrel-like configuration, and the α-rings control substrate entrance via a dynamic gating process (42). As previously demonstrated, the closed conformation of the 20SPT is maintained by a lattice formed by interactions among the N-terminal tails of the α subunits (4, 22). Deletion of the α3 N-terminal domain increased the proteasomal peptidase activity and promoted the opening of the 20SPT gate (22), whereas deletion of both the α3 and α7 N-terminal domains was necessary to increase the 20SPT proteolytic activity (4). The opening of the eukaryotic 20SPT gate can occur concomitant with its coupling to the 19S regulatory particle (28, 49) in a process dependent on specific activators (*e.g.*, yeast Blm10) (12) and on the presence of poly-ubiquitylated substrates (40).

Our hypothesis is that post-translational modifications, including S-glutathiolation, could also control the activity of the free 20SPT pool by regulating the gating process in a manner that is independent of the 19S regulatory particle. The addition of glutathione moieties to proteasomal cysteine (Cys) residues primarily during oxidative challenges has been described in diverse eukaryotic organisms from yeast to plants and mammals (14–16, 35, 46). This post-translational modification of the 20SPT affects its peptidase activities (15, 46) and is reversed by thiol-disulfide oxido-reductases (46). Although S-glutathiolation appears to be a widespread metabolic modification of the 20SPT, neither the identification of the subunits and Cys residues susceptible to S-glutathiolation nor its structural and functional meaning have been elucidated thus far, which is due, in part, to the large number of Cys residues present in this protein complex. Here, we report that 20SPT within cells is under redox regulation by glutathione that affects gate opening and the degradation of oxidized or unstructured proteins. During this process, the 20SPT purified from yeast cells grown to the stationary phase contains 2 out of the 28 analyzed Cys residues modified by a glutathione moiety.

Results

Proteolysis rates are increased when the 20SPT is S-glutathiolated

In a previous work, we showed that the 20SPT isolated from yeast cells grown to stationary phase in a glucose-containing medium was S-glutathiolated (46). This post-translational modification alters the proteasomal site-specific activities (peptidase activity) (14, 15, 46). In the present work, we tested the proteolytic ability of 20SPT in different redox forms: the S-glutathiolated form was obtained from cells grown in YPD medium (referred to as nPT-SG), and the reduced form was obtained by treatment of the nPT-SG samples with 20 mM dithiothreitol (DTT) (referred to as PT-SH). We conducted a set of experiments *in vitro* with the nPT-SG as a model of physiologically S-glutathiolated 20SPT, and we also used similar preparations of PT-SH. Both cores were incubated with proteins known to be degraded by the 20SPT, such as oxidized bovine serum albumin (BSA_{ox}), casein, and glutaredoxin 2 (Grx2). Grx2 was selected because it is either degraded by the 20SPT or poly-ubiquitylated inside yeast cells (46). Moreover, the ability of Grx2 to deglutathiolate the 20SPT concomitant with its degradation has been previously demonstrated (46).

All proteins tested were degraded more extensively by the nPT-SG core than by the PT-SH core (Fig. 1A–C). To quantify the peptide fragments generated by both redox forms, the 20SPT preparations were incubated with either BSA_{ox} derivatized with dinitrophenylhydrazine (BSA_{ox}-DNPH) or fluorescein isothiocyanate (FITC)-modified casein (casein-FITC). The peptides derived from BSA_{ox}-DNPH refer exclusively to the oxidized fragments generated by hydrolysis. The nPT-SG species produced at least twice as many peptides from each substrate (Fig. 2A and B), confirming the proteolysis rate observed by sodium dodecyl sulfate polyacrylamide gel electrophoresis (SDS-PAGE). Control experiments were conducted by incubating proteins known to be resistant to degradation by the 20SPT (Supplementary Fig. S1; Supplementary Data are available online at www.liebertonline.com/ars).

Here, we show that the proteolytic rate for the degradation of these proteins (oxidized, unstructured, and oxidoreductases) increases when acted upon by the S-glutathiolated form of 20SPT (nPT-SG). Because both processes are dependent on the loss of intracellular reductive ability, it is likely that the intracellular pool of oxidized proteins increases concomitantly with proteasomal S-glutathiolation (15). This conclusion is in agreement with the observation that the S-glutathiolated 20SPT more efficiently degraded oxidized proteins (Figs. 1 and 2). We hypothesized here that the redox control of gating is the mechanism that underlies proteolysis by glutathiolated 20SPT. The nPT-SG would prevail on its open-gate conformation and would facilitate the access of protein substrates into the inner catalytic chamber, thereby increasing proteolytic rates.

S-glutathiolation modifies proteasomal gating conformation

To test the hypothesis raised above, we used transmission electron microscopy (TEM) to investigate whether proteasomal gating is modified by thiolation. A high frequency (75% ± 5%) of open structures was observed in the nPT-SG

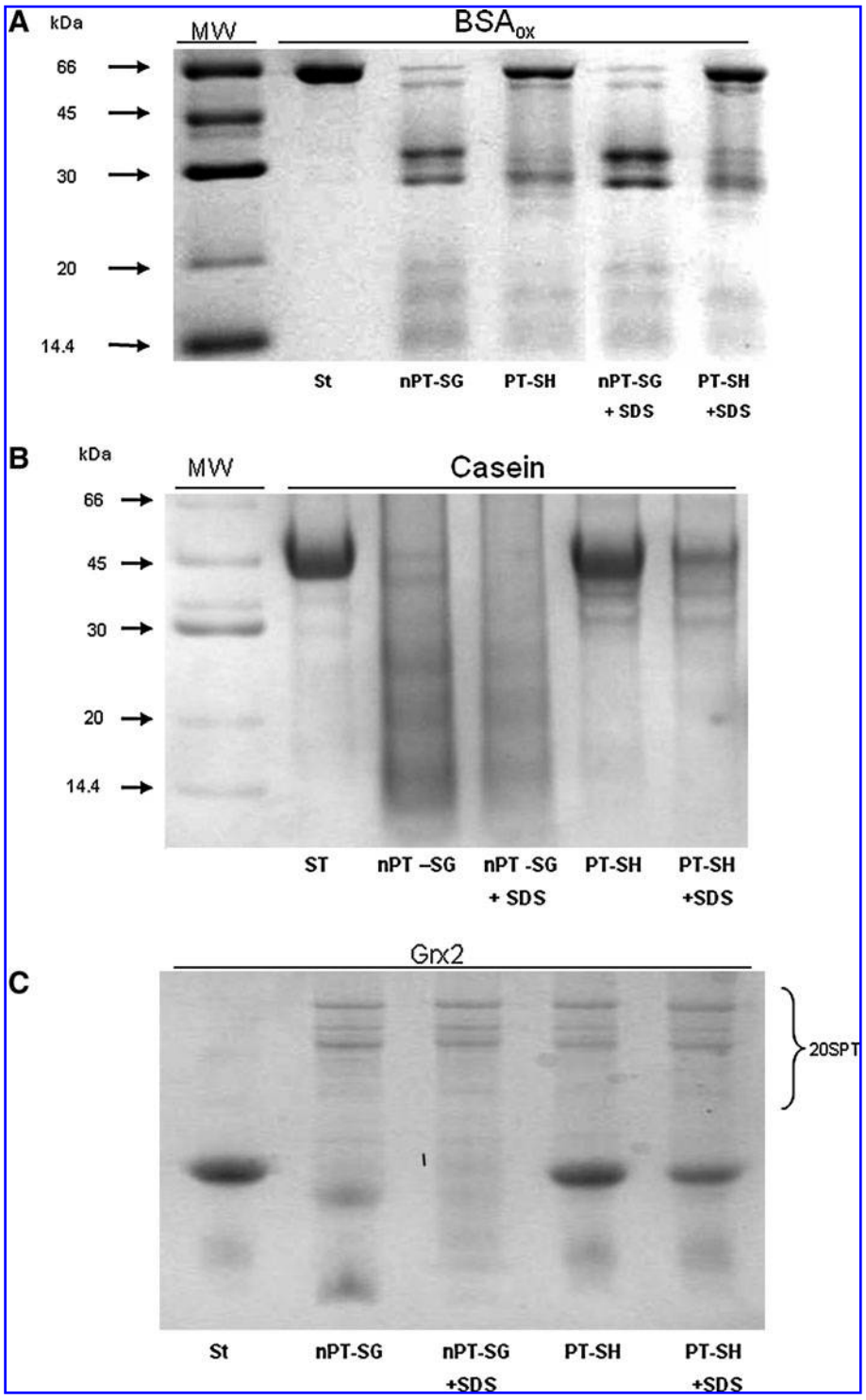

FIG. 1. Protein degradation by redox-modified 20S catalytic unit of the proteasome (20SPT) preparations. Representative sodium dodecyl sulfate polyacrylamide gel electrophoresis (SDS-PAGE) of **(A)** oxidized bovine serum albumin (20 μg; BSA_{ox}), **(B)** casein (20 μg), and **(C)** glutaredoxin 2 (15 μg; Grx2) after incubation for 120, 15, and 60 min, respectively, with natively S-glutathiolated 20S proteasome (5 μg; nPT-SG) and dithiothreitol (DTT)-treated proteasome (5 μg; PT-SH). After this incubation, the samples were filtered through YM-100 microfilters (Millipore) to remove the 20SPT, and the filtrates were used to load the gels. To test the integrity of the preparations, 0.0125 % SDS-containing buffer (+SDS) was utilized as a positive control. BSA was oxidized in the presence of 5 mM H_2O_2 and 100 μM diethylene triamine pentaacetic acid (DTPA) for 30 minutes at room temperature, and the remaining H_2O_2 was removed by cycles of filtration and redilution through YM-10 microfilters (Millipore). All incubations were performed at 37°C. St, standard proteins not incubated with 20SPT; MW, molecular weight standard.

samples (Fig. 3A and Supplementary Fig. S2A), whereas after treatment with DTT (20 mM), the frequency of closed particles predominated and represented approximately 90% ± 10% of the total complexes (Fig. 3B and Supplementary Fig. S2B). Our results are in agreement with reports in the literature that demonstrate the dynamic state of the proteasomal gate (36, 41, 47).

As a complementary and independent assessment of the overall dimensions of the proteasome, small-angle X-ray scattering (SAXS) experiments were performed. According to the results obtained (Table 1 and Supplementary Data), there is a significant three-dimensional (3D) structural shift between both redox forms of the 20SPT, which is in agreement with the TEM data already discussed. For both 20SPT redox forms, the SAXS data indicated a cylindrical shape of the particles with an internal hole. The outer diameter decreased from 106 Å (nPT-SG) to 72 Å when identical preparations were treated with DTT (PT-SH).

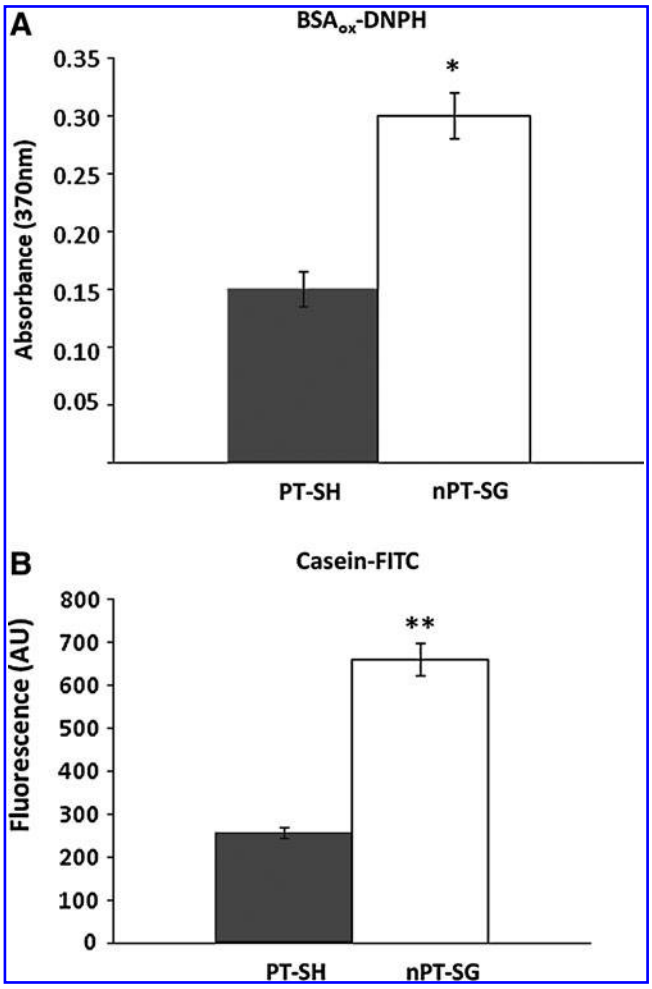

FIG. 2. Quantitative protein degradation by redox-modified 20SPT preparations. (A) BSA_{ox} that had reacted with dinitrophenylhydrazine (DNPH), a carbonyl protein reactant (31), was incubated with the 20SPT preparations for 60 min followed by the addition of 20% trichloroacetic acid. The supernatant was retained for spectrometric measurement at 370 nm. **(B)** Fluorescein isothiocyanate (FITC)-modified casein (casein-FITC) was incubated with the proteasomal preparations for 15 min followed by the addition of 20% trichloroacetic acid. The supernatant was sampled for fluorometric determination (excitation, 492 nm; emission, 515 nm). Both the casein-FITC and DNPH-treated BSA_{ox} samples were processed using the same conditions in the absence of the proteasome as controls. The results shown represent the mean ± SD and are expressed as arbitrary units of absorbance (hydrazone adducts) or fluorescence (FITC). *$p < 0.000021$; **$p < 0.000003$.

Remarkably, the inner diameter was almost completely closed in the PT-SH samples (Table 1), confirming the data visualized by TEM (Fig. 3B). The shift from the open to the closed conformation was previously demonstrated to be accompanied by slight changes in the outer diameter and length (37). The proteasomal lengths and diameters obtained by SAXS are in agreement with data in the literature (Supplementary Table S1). However, the inner diameter measured in the present work (80 Å; nPT-SG) is higher than that determined by the few crystallographic studies that have been performed or evaluated by TEM (Supplementary Table S1). A comparative revision of the 20SPT dimensions is presented in the Supplementary Data section (Supplementary Table S1).

Only Cys residues of the α subunits were observed to be modified by glutathione

Because S-glutathiolation strongly affects both the ability of the 20SPT to degrade oxidized/unstructured proteins and its gate conformation, it was necessary to identify the Cys residues that were post-translationally modified in both nPT-SG and PT-SH. Therefore, we initially isolated and characterized the 20SPT subunits by two-dimensional electrophoresis (2-DE) coupled to MALDI-TOF fingerprinting (Supplementary Fig. S3, Supplementary Table S2). Next, the Cys-containing 20SPT subunits were digested with trypsin and prepared for liquid chromatography–tandem mass spectrometry (LC-MS/MS) analysis. Two S-glutathiolated Cys residues (Cys76 and Cys221) in the α5 subunit were identified in the nPT-SG by tandem mass spectrometry analysis. To better characterize all of the Cys residues that are potentially prone to S-glutathiolation, the purified nPT-SG preparations were treated *in vitro* with 10 mM glutathione (GSH). In this series of experiments, we identified two other subunits (α6 and α7) in addition to the α5 subunit and a total of seven GSH-modified Cys residues (+305.1 Da) among the 35 Cys residues present in mature yeast 20SPT (Table 2; Fig. 4A). The samples that were reduced by DTT (PT-SH) were subjected to LC-MS/MS analysis as a control (Fig. 4B). The latter preparations did not present any glutathione-modified Cys residues. We cannot discard the possibility that the β subunits were also modified by S-glutathiolation because we did not succeed in identifying seven of the Cys-containing fragments in the β subunits among the 20 predicted. Nevertheless, all of the Cys-containing fragments in the α subunits were identified (Supplementary Table S3). This 2-DE/mass spectrometry analysis was employed at least five times with reproducible results.

As expected from the heterogeneous proteasome population (nPT-SG preparations), the Cys residues were observed in different oxidative states as follows: reduced (-SH, which were modified by iodoacetamide), modified via S-glutathiolation or hyper-oxidized to sulfinic acid (Cys-SO_2H) (Supplementary Table S3). Remarkably, Cys-SO_2H was detected in all of the Cys residues (except Cys66 from the α6 subunit) prone to S-glutathiolation (Supplementary Table S3), indicating that the formation of Cys sulfenic acid (Cys-SOH) is a common intermediate in both processes (hyper-oxidation and S-glutathiolation). In fact, we have previously shown that 20SPT S-glutathiolation occurs via a Cys-SOH intermediate (15). It is likely that the thiolate form of the Cys-sulfur atom (RS^-) would be the most prone to oxidation (53) to sulfenic acid because this anion is a stronger nucleophile than its protonated counterpart. A low pK_a of the thiol group and solvent accessibility are important factors for increasing the thiol protein reactivity.

Given the location of the S-glutathiolated Cys residues in the 3D structure of the 20SPT, Cys221 from the α5 subunit is the only modified residue whose thiol group is highly accessible to the solvent (Fig. 5A; Supplementary Fig. S 4A and B). Furthermore, the environment around Cys221 allows for the docking of a GSH molecule (Fig. 4B and Supplementary Fig. S4C) that fits very well into the proteasomal bulk where GSH-charged groups (both N- and C-terminal carboxyl groups and the N-terminal amine) can establish important

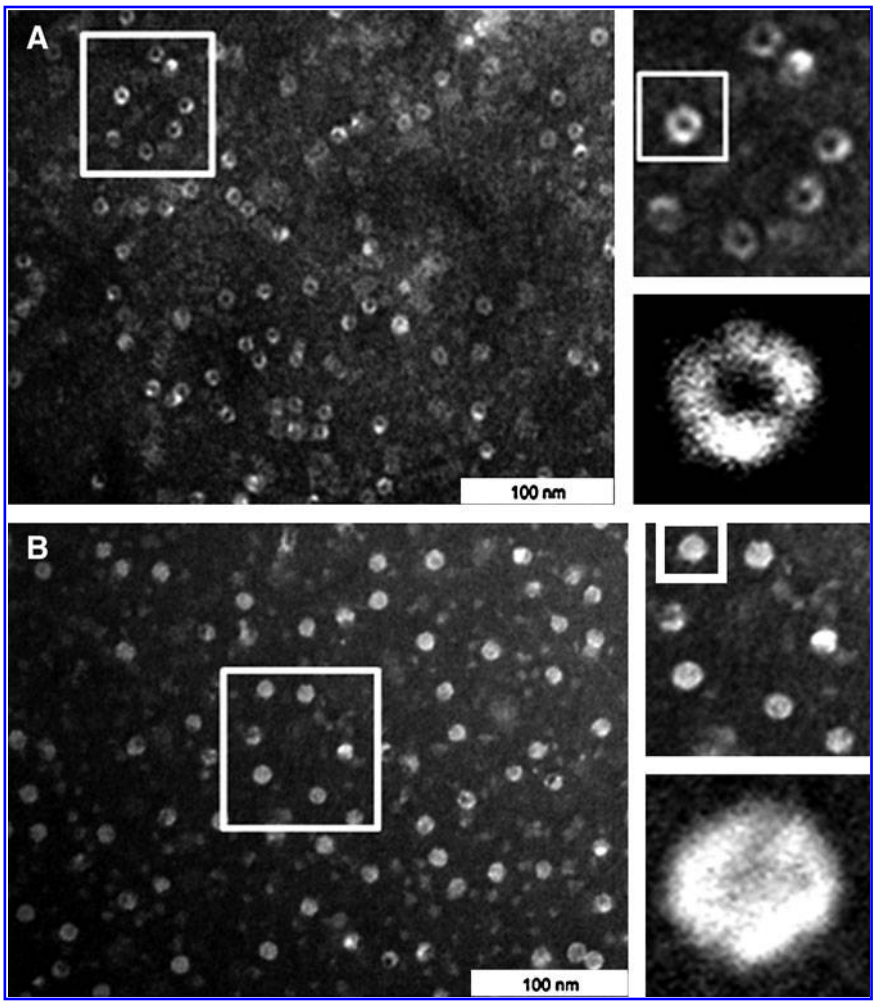

FIG. 3. 20S proteasomal gating control is dependent on the cysteine (Cys) redox state. (A) Representative images obtained by transmission electron microscopy of nPT-SG in the open conformation. **(B)** nPT-SG samples analyzed immediately after treatment with 20 mM DTT for 30 min followed by a washing procedure to eliminate DTT, as described in the Materials and Methods section. The squares were amplified as shown on the right. The combined conformations (open and closed) were observed in both 20SPT preparations (nPT-SG and PT-SH), as shown in Supplementary Fig. S1A and B (Supplementary Data).

saline interactions with charged groups of the side chains of proteasomal residues (E197, Q225, K229, and K235; Fig. 5B). In the case of Cys76, the other natively S-glutathiolated residue, no docking was obtained, likely because the thiol group is not located on the protein surface. It is probable that the S-glutathiolation of Cys76 is dependent on structural changes that allow the reaction of GSH with the thiol group to occur. Remarkably, Cys76 is fully conserved among the 20SPT α5 subunits from yeast, plants and mammals (Supplementary Fig. S5).

S-glutathiolation promotes the allosteric modification of site-specific proteasomal activity

The increased degradation of proteins by nPT-SG may appear contradictory to our previous finding that S-glutathiolation of the 20SPT partially inhibited the chymotrypsin-like (ChT-L) and post-acidic proteasomal activities, which were measured using fluorogenic peptides (15, 46) (see Supplementary Table S4). Our hypothesis is that, in addition to affecting gating, S-glutathiolation also promotes an allosteric modification of the proteasomal catalytic sites. In fact, according to SAXS analysis (Table 1), the 20SPT conformation experienced changes not only in its outer and inner diameters but also in its longitudinal length depending on its redox state. To address this hypothesis, we performed experiments with the mutated 20SPT lacking the N-terminal sequences of its α3 and α7 subunits. As reported (3), this mutated form of the 20SPT is permanently in its open conformation and is highly active compared with the wild-type 20SPT. These results were reproduced in our lab (not shown). We then performed a series of experiments with purified preparations of the mutated (ΔNα3α7) 20SPT to evaluate whether thiol reactants would modify its activity, as had been observed in the case of the wild-type 20SPT (15). Either dimedone (sulfenic acid reactant), 7-chloro-4-nitrobenzo-2-oxa-1,3-diazole (NBD; sulfhydryl and sulfenic acid reactant), or oxidized glutathione (GSSG; sulfhydryl reactant) promoted the inhibition of the ChT-L ΔNα3α7 20SPT activity (Table 3), which could not be explained by changes in the diameter of the 20SPT gate but could be related to changes in the length of this core particle (Supplementary Table S1). In the context of this work, emphasis should be placed on the conditions that initially resulted in the 20SPT-Cys-SOH form that is equivalent to that formed by the oxidation of the ΔNα3α7 20SPT with 5 mM H_2O_2 in the presence of diethylene triamine pentaacetic acid (DTPA; to avoid unspecific oxidation by contaminant metals) followed by incubation at increasing GSH concentrations. The ChT-L ΔNα3α7 20SPT activity was inhibited in a dose-dependent manner by GSH (Table 3). Next, we performed SAXS analyses of the ΔNα3α7 20SPT preparations to evaluate whether treatment with 1 mM GSH modifies the proteasome conformation. No alteration in either the external or internal diameters was detected by comparing samples incubated with GSH or DTT,

Table 1. Proteasomal Surface Dimensions Obtained From Small-Angle X-Ray Scattering Measurements

Parameters	*nPT-SG*	*PT-SH*
Outer diameter (Å)	106 ± 4	72 ± 4
Pore diameter (Å)	78 ± 4	0 to 10
σ (Å)	5	5
Length L (Å)	188 ± 20	210 ± 40
χ^2	2.5	3.5

although the maximum length of the ΔNα3α7 20SPT was 210 nm in the sample incubated with GSH and 230 nm in the absence of GSH (Supplementary Table S1). These results indicated that partial inhibition of the ChT-L peptidase activity is most likely related to an allosteric phenomenon triggered by S-glutathiolation, which involves changes in the length of 20SPT that are distinct from the gating.

Discussion

Collectively, the present results demonstrate that the S-glutathiolated 20SPT exhibits higher degradation rates of oxidized and partially unstructured proteins, most likely because of its gate opening. Based on our results, we hypothesize that the opening of the catalytic chamber, which is triggered by the thiolation of the proteasomal α5 subunit, would facilitate the ability of cells to cope with misfolded proteins without requiring ATP. It is likely that the 20SPT plays a prominent role in the response to oxidative stress because various reports have demonstrated that ATP has no stimulating effect on the degradation of oxidized proteins in cell lysates (44). Accordingly, Davies and colleagues (45) concluded that oxidized proteins are degraded by the 20S proteasome in a manner independent of both the 19S regulator and, consequently, ubiquitin by demonstrating that the disruption of the ubiquitylation system did not impair the degradation of oxidized proteins.

According to some reports (10, 22, 26), the so-called latent form of the free 20SPT is closed. However, in reports describing the gating of the 20SPT (yeast and human 20SPT), a mixed pool of open and closed conformations is observed (2, 21, 29, 36–38). Notably, in the protocols described in the literature, DTT is present in the purification procedure at low concentrations (0.1–2 mM), which would not remove the glutathionyl moiety from the 20SPT. Among the DTT concentrations used in our experiments (not shown), a minimum of 20 mM was necessary for alteration of the gating (Fig. 3B, Table 1) to occur concomitantly with the disappearance of the glutathione-modified Cys residues (Fig 4B). As previously demonstrated, the reduction of the 20SPT inside cells may be accomplished by oxidoreductases (46).

Glutathiolation is emerging as a relevant post-translational modification that is involved in redox regulation. In several proteins under redox control by glutathiolation, only one or very few Cys residues are involved (34). In the case of the redox process mediated by peroxides, it is also expected that few Cys residues exhibit high reactivity toward this oxidant (53). Once reactive protein thiols are oxidized to sulfenic acid, they can more easily undergo further reactions, such as hyperoxidation to sulfinic or sulfonic acids and S-glutathiolation and the formation of intra- and interprotein disulfides or sulfenylamide derivatives (53). Notably, depending on the thiol location in the protein (pK_a; solvent accessibility) and the cellular compartment of a given protein, the peroxide-sensitive thiol targets may be directly oxidized without disruption to the overall redox homeostasis. Therefore, the finding that only 2 of the 28 Cys residues detected in the 20SPT were S-glutathiolated indicates that this post-translational modification may represent a redox signaling process. In fact, it appears that there is a microenvironment appropriate for GSH binding in the vicinity of Cys221 from the α5 subunit (Fig. 5B). The other glutathiolated Cys residue (Cys76) is fully conserved among all of the α5 subunits analyzed (Supplementary Fig. S5), suggesting a prominent role for this amino acid. Additionally, Cys42 from the α7 subunit (S-glutathiolated *in vitro*) is highly conserved (Supplementary Fig. S5).

Interestingly, the activity and gating of the vascular K_{ATP} channel are also modulated by the S-glutathiolation of a single

Table 2. 20S Proteasome S-Glutathiolated Cysteine Residues

Subunits - position	*Cys-SG*	*Peptide sequence*	*Monoisotopic ion [M+H]+GSH*	m/z *ratio detected*	*Error (ppm)*
PT-SG					
α5					
73–86	Cys76	R.HIGCAMSGLTADAR.S	1707.728	569.914	17.5
94–122	Cys117	R.TAAVTHNLYYDEDINVESLTQSVCDLALR.F	3558.638	890.415	11.2
212–224	Cys221	K.LDENNAQLSCITK.Q	1753.778	585.264	11.4
α6					
66–82	Cys66	K.CDEHMGLSLAGLAPDAR.V	2060.888	687.634	9.7
α7					
42–52	Cys42	K.CNDGVVFAVEK.L	1485.638	743.322	6.7
73–86	Cys76	R.HIGCVYSGLIPDGR.H	1791.818	597.944	11.1
nPT-SG					
α5					
73–86	Cys76	R.HIGCAMSGLTADAR.S	1707.81	569.94	52.7
206–224	Cys221	K.QVMEEKLDENNAQLSCITK.Q	2513.10	1257.62	35.8

The 20SPT preparations were treated with 10 mM GSH (PT-SG) or were natively S-glutathiolated (nPT-SG). All subunits containing Cys residues identified on the two-dimensional electrophoresis gel coupled to MS-fingerprinting were digested with trypsin followed by an LC-Q-ToF-MS analysis.

GSH, glutathione; PT-SG, *in vitro* S-glutathiolated 20S proteasome.

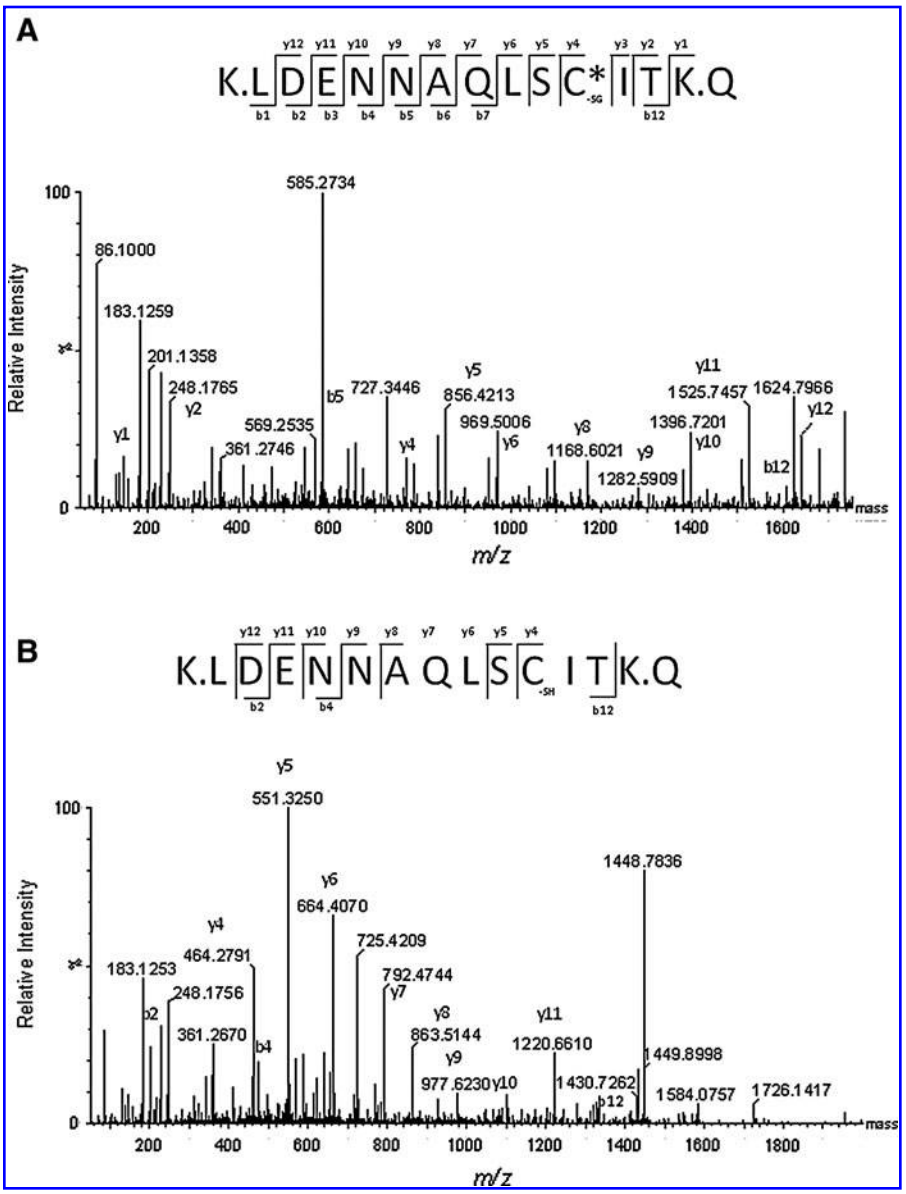

FIG. 4. Representative spectra of the thiol-modified proteasomal Cys residues obtained by LC-ESI-MS/MS. LC-ESI-Q-TOF (Waters Synapt HDMS) analysis of the tryptic peptide from the 20SPT α5 subunit containing Cys221. (A) MS/MS spectrum of a triply charged ion $[M+3H]^{3+}$ with an *m/z* ratio of 585.28 containing a glutathione moiety (+305.1) attached to the Cys residue. The monoisotopic mass of the deprotonated peptide (LDENNAQLSCITK) is equal to 1752.82 Da. **(B)** MS/MS spectrum corresponding to the same peptide shown in **A** from DTT-treated samples. The doubly charged ion $[M+2H]^{2+}$ possesses an *m/z* ratio of 724.84 and a monoisotopic mass of 1447.67 Da, indicating the reduced form of the Cys residue. The respective fragmentation series is shown above each spectrum.

Cys residue (Cys176 residue) within the Kir6.1 subunit (54). In this case, glutathiolation stabilizes the gate in its closed conformation.

We report for the first time a proteasomal post-translational modification that modifies the gate opening of the 20SPT, thereby regulating the ability of the 20SPT to degrade target proteins. Our results suggest a need to reevaluate the fundamental aspects of the currently favored models of the regulation of proteasomal gating based on the destabilization of the N-termini of the α3 and α7 subunits (3, 4, 22). The latter model summarizes the important dynamics of the α subunits that contribute to gating control upon assembly of the 26S proteasome, but it does not explain the mechanism that triggers such dynamics of the free 20SPT pool. The mechanism described here was shown to be closely associated with the intracellular redox status because cells growing in a less oxidative environment possess proteasomes with low levels of S-glutathiolation (46), which corresponds to a population of core particles in the reduced state and with closed gates. The present model agrees with the idea that during the oxidant-mediated damage of proteins, degradation may be facilitated inside cells to avoid energy consumption. The mechanism by which oxidized proteins interact with the 20SPT particle for degradation is unknown. A loss of secondary structure and the consequent increase in the exposure of hydrophobic patches has been claimed as the phenomena underlying this process (5, 19, 39, 44). We propose that the redox modification of the 20SPT under oxidative conditions would facilitate the proteolytic processing of unstructured proteins, including oxidized proteins. The critical function of the proteolytic systems in maintaining a continuous turnover of all intracellular proteins, including those that are still functional, is necessary to prevent the accumulation of intracellular damage and its associated consequences. This function represents an important aspect of protein quality control. Limiting the half-life of the cellular proteins reduces their chances of damage and avoids their risk for aggregation.

The proteasome plays a very important role in the clearance of the majority of proteins implicated in neurodegenerative processes (43). Because intracellular inclusions that are

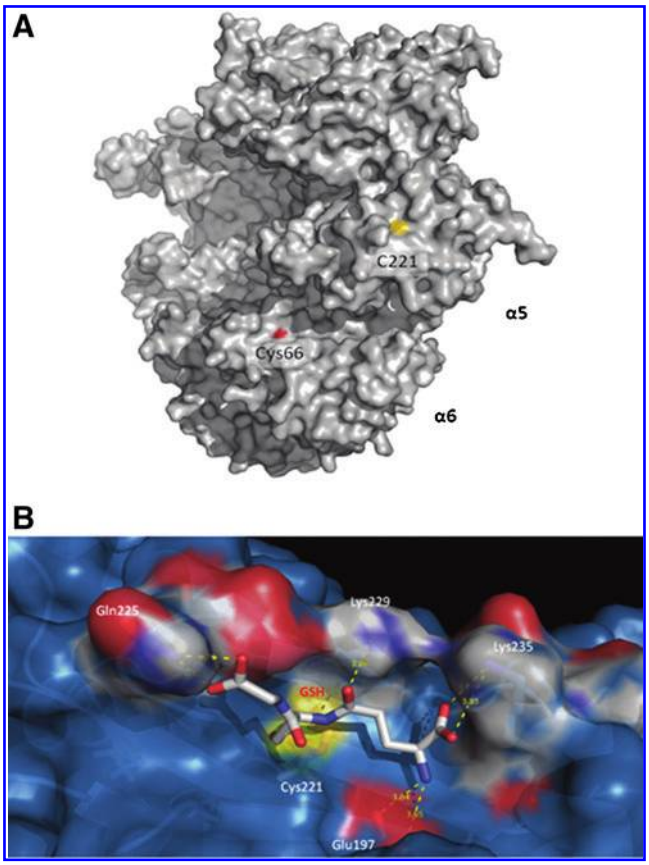

FIG. 5. Location of Cys221 in the α5 subunit in the 3D proteasomal structure. (A) Surface structure of the α-ring highlighting the solvent-accessible sulfur atom (yellow) of Cys221 from the α5 subunit and the surface oxygen (red) from the Cys66 residue of the α6 subunit. **(B)** Modeling of glutathione docking onto Cys221 of the α5 subunit was performed by Gold 4.1–Protein-Ligand Docking (Cambridge Crystallographic Data Centre). The proteasome is shown by a surface representation, and the glutathione is represented by sticks. The proteasomal residues interacting with the GSH-charged groups are highlighted in white in the surface representation and are depicted as blue sticks underneath. The sulfur atoms are depicted in yellow. The distances (Å) between the GSH-charged groups and the lateral chains of the proteasomal amino acids are shown. The graphical images were generated using Pymol software (DeLano Scientific).

derived from protein aggregation and associated with neurodegenerative diseases are rich in ubiquitylated proteins, it is assumed that ubiquitin-proteasome system (UPS) impairment is associated with the etiology of these pathologies (6, 11, 43). Thus, UPS has been investigated extensively in many neurodegenerative diseases. In fact, there are data suggesting that the mono-ubiquitylation of protein aggregates is an important signal to remove aggregates via autophagy (18, 27). However, processes favoring the ubiquitin-independent removal of oxidized or unstructured proteins that are prone to aggregation appear to also be an immediate and important mechanism to avoid neurotoxicity. In fact, the 20SPT directly interacts with the prion protein (8), soluble oligomers, and insoluble filaments of α-synuclein or amyloid-Aβ peptide aggregates (32, 55). Additionally, monomeric α-synuclein

Table 3. ChT-L Activity of Purified Preparations of the ΔNα3α7 20SPT After Treatment With Sulfhydryl Reactants

Control	100 ± 5
Dimedone (mM)	
10	85 ± 4.5
20	60 ± 5
NBD (μM)	
50	65 ± 6
100	49 ± 5
GSSG (mM)	
5	80 ± 6.5
10	60 ± 4
GSH (mM)[a]	
1	91 ± 5
2.5	79 ± 5.5
5	40 ± 4

The ΔNα3α7 20SPT was purified from cells grown to stationary phase in YPD medium. The assays were performed with 10 μg 20SPT pre-incubated with the reactants for 10 min followed by the addition of 65 μM succinyl-Leu-Leu-Val-Tyr-MCA. The results are expressed as a percentage of the control samples, which are set at 100.

[a]The purified ΔNα3α7 20SPT was oxidized with 5 mM H_2O_2 in the presence of 100 μM DTPA. After H_2O_2 washing, the oxidized samples were reacted with GSH at increasing concentrations, as shown. In all experiments, the reactants were removed by cycles of filtration and re-dilution prior to the next step.

NBD, 7-chloro-4-nitrobenzo-2-oxa-1,3-diazole; GSSG, oxidized glutathione.

is easily degraded by the 20S proteasome in a ubiquitin-independent manner (33, 50). Therefore, the redox regulation process described here represents an important aspect of protein quality control.

Proteasomal S-glutathiolation is a reversible and protective mechanism that allows for the removal of unstructured and oxidatively damaged proteins. Because either hyperoxidation or complexation to metals of proteasomal Cys residues would preclude S-glutathiolation and, thus, gate opening, one would predict deleterious consequences from the accumulation of proteins prone to aggregation in a highly oxidative environment. Accordingly, irreversible proteasome oxidation (9) and metal accumulation (17) are described in the brain of Alzheimer's patients together to proteasome impairment.

According to the present results, the increased proteolysis rates due to proteasomal S-glutathiolation are primarily dependent on the 20SPT gate opening despite the partial inhibition of site-specific activity. According to another line of investigation in our laboratory, the peptide fragments originating from degradation of identical proteins differ in their cleavage sites depending on the proteasomal redox status, including the generation of immune-competent fragments (unpublished). Similar to the case of the immuno- and thymoproteasomes in their specific contexts, the redox modification of the standard proteasome might play an important role in the regulation of cell redox signaling.

Materials and Methods

Materials

Bovine serum albumin, casein, casein-FITC, cytochrome c, DTPA, dimedone, DTT, GSH, and NBD were purchased from Sigma-Aldrich (St. Louis, MO). The fluorogenic substrate succinyl-Leu-Leu-Val-Tyr-MCA was purchased from

Calbiochem (Merck, Darmstadt, Germany). The molecular weight markers for SDS-PAGE and ATP were purchased from GE Biosciences (GE Healthcare Europe, Glattbrugg, Switzerland). The Bradford protein assay reagent was purchased from Bio-Rad (Hercules, CA).

Yeast strain and growth

The *Saccharomyces cerevisiae* RJD1144/JD 122 (MATa his3(200 leu2-3,112, lys2-801 trp1(63 ura3-52 $PRE1^{FH}$ ::Ylplac211 URA3) strain, derived from the JD47-13C strain, was kindly donated by Dr. Raymond Deshaies (Division of Biology, Caltech, Pasadena, CA). The RJD1144 strain contained the 20S proteasome PRE1 gene modified with the FLAG peptide and a poly-histidine tail sequence (51). The cells were cultured in YPD medium containing 4% glucose (referred to as YPD) at 30°C with reciprocal shaking and harvested after 60 h of incubation. The SUB556 strain, derived from SUB62, was kindly donated by Dr. Michael H. Glickman (Department of Biology, Technion-Israel Institute of Technology, Haifa, Israel). The 20SPT from the SUB556 strain contains N-terminal deletions in both the α3 and α7 subunits (3).

Extraction and purification of the 20S proteasome

The 20SPT from the RJD1144 strain was purified by nickel affinity chromatography with a continuous gradient of imidazole using high performance liquid chromatography (Akta Purifier, GE Healthcare). Neither DTT nor any other thiol reductant was utilized in any step of the entire purification procedure, which differs from nearly all other protocols described in the literature to date. The final preparations were passed through a PD10-desalting column according to the manufacturer's protocol (GE Biosciences). The untagged 20SPT from the RJD1144 strain and the ΔNα3α7 20SPT from the SUB556 strain were purified by conventional chromatography (14). The untagged 20SPT was utilized as a control relative to the tagged sample.

Reduction and S-glutathiolation of the 20S proteasome

When specified, the preparations of the purified 20SPT (1 mg) extracted from cells grown in YPD-rich medium were incubated overnight at 4°C with 300 mM DTT. Following this incubation, the proteasome preparations were passed through a PD10-desalting column according to the manufacturer's protocol (GE Biosciences) to remove the DTT, imidazole, and NaCl. The eluted protein fractions were tested for the presence of DTT via the reaction with 75 μM 5,5′-dithiobis-(2-nitrobenzoic acid)(DTNB; also known as Ellman's reagent). Only protein fractions in which no DTT was detected were selected for further procedures. These preparations are herein referred to as the DTT-reduced 20SPT (PT-SH). To obtain the *in vitro* S-glutathiolated protein (PT-SG), aliquots of the native 20SPT (nPT-SG) were incubated at room temperature for 20 min in the presence of 10 mM GSH in 50 mM Tris buffer, pH 7.5. Following the incubation, GSH was removed by cycles of centrifugation and rediluted through YM-100 microfilters. After the determination of the protein concentration, aliquots of the PT-SH and PT-SG preparations were selected for additional assays.

PAGE analysis of proteins

SDS-PAGE was performed as previously described (7). After incubation at the indicated conditions (Fig. 1), the protein preparations were mixed with gel loading buffer (100 mM Tris-HCl [pH 6.8], 10% glycerol, 2% SDS, and 0.02% bromophenol blue) and applied to the gel.

Liquid chromatography-quadrupole-time of flight mass-spectrometry identification of S-glutathiolated cysteinyl residues

The trypsin-digested products were analyzed by LC-MS/MS in a Synapt HDMS instrument (Waters, Millford, MA) coupled online to a nanoAcquity ultra performance liquid chromatography system. The digests were loaded and desalted using a 180-μm × 20-mm Waters Symmetry C18 column. After the desalting step, the samples were directed to a 100-μm × 100-mm Waters BEH130 C18 column at a flow rate of 1.0 μL/min. Mobile phases A and B consisted of 0.1% formic acid/water and 0.1% formic acid/acetonitrile, respectively. The gradient conditions used were as follows: at 0 min the concentration of B started at 3% and increased linearly to 30 % in 20 min; the concentration of B then increased up to 70% in 40 min and remained at this level until 50 min; finally, in the next minute, the concentration decreased to 3%. The typical operating conditions of the mass spectrometer in the data-dependent analysis experiments were as follows: capillary voltage, 3.0 kV; cone voltage, 40 V; power supply temperature, 100°C; and collision energy, 6 and 4 eV in the Trap and Transfer in the MS mode. The collision energy was selected as a function of the precursor charge and the *m/z* value. The instrument was externally calibrated using phosphoric acid oligomers over an *m/z* range of 100 to 3000.

Negative staining of the 20SPT particles by TEM

Drops (12 μL) of the purified 20SPT preparations (0.5 μg/μL) were applied onto carbon-coated 400 mesh copper grids. After 1 min the excess liquid was blotted with a tissue paper, leaving a small amount of residual fluid. Negative staining was performed with 12 μL of 2% phosphotungstic acid, pH 7.2, for 10 s and then the samples were blotted dry. The grids were examined in an LEO 906E transmission electron microscope (Zeiss, Germany) at an acceleration voltage of 100 kV. The images were acquired using a CCD camera MegaView III in conjunction with the *iTEM* - Universal TEM Imaging Platform software (Olympus Soft Imaging Solutions GmbH, Germany). Our protocol did not consider the side-on view of the 20SPT; thus, we did not utilize a vacuum to prepare the grids (Dr. Edward Morris, personal communication). A quantitative analysis was manually performed by counting the frequency of open or closed structures from identical proteasomal populations. The possibility of saturated images was excluded because the microscope was operated under similar light conditions and also because many of the images obtained showed both closed and open conformations together, as shown in Supplementary Fig. S2A and B.

Small-angle X-ray scattering

The SAXS experiments were performed using Bruker Nanostar™ equipment (Karlsruhe, Germany). The data were collected at room temperature using samples of the

nPT-SG, PT-SH (both at 2.2 mg/mL), and ΔNα3α7 20SPT (0.7–1 mg/mL) resuspended in 20 mM Tris/HCl, pH 7.5, buffer. The measurements were obtained using samples placed in reusable quartz capillaries glued on stainless steel cases, which allowed for the measurement of both the samples and the background under the same conditions. Several 1-h frames were taken to enable the monitoring of the sample stability. The data treatment, background subtraction and frame average were performed using the SUPERSAXS program package (Oliveira and Pedersen, unpublished). The complete methodology and data analysis are described in Supplementary Data.

GRID methodology

The GRID methodology (20) was utilized for the docking analysis of the glutathione (GS-) that was covalently attached to Cys residues of the proteasome. The 3D structure of the yeast 20SPT was obtained from the PDB file 1RYP (resolution: 2.4 Å) (23). The side chains of the glutathione and proteasomal residues were placed in their lowest energy positions, and their energies were minimized using the Tripos force field with Pullman charges and conjugate gradient minimization, keeping all other protein residues rigid. The modeling of glutathione docking was performed on Gold–Protein-Ligand Docking (Cambridge Crystallographic Data Center), and all graphical images were generated using Pymol software (DeLano Scientific).

Acknowledgments

We thank Dr. Kelvin J.A. Davies and Dr. Ohara Augusto for their critical reading of the present work. We are grateful to Dr. Alberto Malvezzi and Dr. Sylvia Carneiro who helped with the structural modeling and the electron microscopy studies, respectively. We thank Adrian Hand for technical support. This work was supported by Fundação de Amparo a Pesquisa do Estado de São Paulo (FAPESP, Grants 08/06731-9 and 07/58147-6) and Instituto Nacional de Ciência, Tecnologia e Inovação de Processos Redox em Biomedicina (Redoxome, CNPq, FAPESP, CAPES).

Author Disclosure Statement

The authors declare no conflict of interest.

References

1. Asher G, Reuven N, and Shaul Y. 20S proteasomes and protein degradation "by default". *Bioessays* 28: 844–849, 2006.
2. Babbitt SE, Kiss A, Deffenbaugh AE, Chang YH, Bailly E, Erdjument-Bromage H, Tempst P, Buranda T, Sklar LA, Baumler J, Gogol E, and Skowyra D. ATP hydrolysis-dependent disassembly of the 26S proteasome is part of the catalytic cycle. *Cell* 121: 553–565, 2005.
3. Bajorek M, Finley D, and Glickman MH. Proteasome disassembly and downregulation is correlated with viability during stationary phase. *Curr Biol* 13: 1140–1144, 2003.
4. Bajorek M, and Glickman MH. Keepers at the final gates: regulatory complexes and gating of the proteasome channel. *Cell Mol Life Sci* 61: 1579–1588, 2004.
5. Baugh JM, Viktorova EG, and Pilipenko EV. Proteasomes can degrade a significant proportion of cellular proteins independent of ubiquitination. *J Mol Biol* 386: 814–827, 2009.
6. Bingol B, and Sheng M. Deconstruction for reconstruction: the role of proteolysis in neural plasticity and disease. *Neuron* 69: 22–32, 2011.
7. Bollag DM, and Edelstein SJ. *Protein Methods*. New York: Wiley-Liss, 1991.
8. Cecarini V, Bonfili L, Cuccioloni M, Mozzicafreddo M, Angeletti M, and Eleuteri AM. The relationship between the 20S proteasomes and prion-mediated neurodegenerations: potential therapeutic opportunities. *Apoptosis* 15: 1322–1335, 2010.
9. Cecarini V, Ding Q, and Keller JN. Oxidative inactivation of the proteasome in Alzheimer's disease. *Free Radic Res* 41: 673–680, 2007.
10. Coux O, Tanaka K, and Goldberg AL. Structure and functions of the 20S and 26S proteasomes. *Annu Rev Biochem* 65: 801–847, 1996.
11. Cuervo AM, Wong ES, and Martinez-Vicente M. Protein degradation, aggregation, and misfolding. *Mov Disord* 25 Suppl 1: S49–54, 2010.
12. Cunha FM, Demasi M, and Kowaltowski AJ. Aging and calorie restriction modulate yeast redox state, oxidized protein removal, and the ubiquitin-proteasome system. *Free Radic Biol Med* 51:664–670, 2011.
13. Dange T, Smith D, Noy T, Rommel PC, Jurzitza L, Legendre A, Finley D, Goldberg AL, and Schmidt M. Blm10 promotes proteasomal substrate turnover by an active gating mechanism. *J Biol Chem*, 2011 [Epub ahead of print].
14. Demasi M, Shringarpure R, and Davies KJ. Glutathiolation of the proteasome is enhanced by proteolytic inhibitors. *Arch Biochem Biophys* 389: 254–263, 2001.
15. Demasi M, Silva GM, and Netto LE. 20 S proteasome from *Saccharomyces cerevisiae* is responsive to redox modifications and is S-glutathionylated. *J Biol Chem* 278: 679–685, 2003.
16. Dixon DP, Skipsey M, Grundy NM, and Edwards R. Stress-induced protein S-glutathionylation in Arabidopsis. *Plant Physiol* 138: 2233–2244, 2005.
17. Duce JA, and Bush AI. Biological metals and Alzheimer's disease: implications for therapeutics and diagnostics. *Prog Neurobiol* 92: 1–18, 2010.
18. Engelender S. Ubiquitination of alpha-synuclein and autophagy in Parkinson's disease. *Autophagy* 4: 372–374, 2008.
19. Ferrington DA, Sun H, Murray KK, Costa J, Williams TD, Bigelow DJ, and Squier TC. Selective degradation of oxidized calmodulin by the 20 S proteasome. *J Biol Chem* 276: 937–943, 2001.
20. Goodford PJ. A computational procedure for determining energetically favorable binding sites on biologically important macromolecules. *J Med Chem* 28: 849–857, 1985.
21. Gregori L, Hainfeld JF, Simon MN, and Goldgaber D. Binding of amyloid beta protein to the 20 S proteasome. *J Biol Chem* 272: 58–62, 1997.
22. Groll M, Bajorek M, Kohler A, Moroder L, Rubin DM, Huber R, Glickman MH, and Finley D. A gated channel into the proteasome core particle. *Nat Struct Biol* 7: 1062–1067, 2000.
23. Groll M, Ditzel L, Lowe J, Stock D, Bochtler M, Bartunik HD, and Huber R. Structure of 20S proteasome from yeast at 2.4 A resolution. *Nature* 386: 463–471, 1997.
24. Grune T, Catalgol B, Licht A, Ermak G, Pickering AM, Ngo JK, and Davies KJA. HSP70 mediates dissociation and reassociation of the 26S proteasome during adaptation to oxidative stress. *Free Rad Biol Med* 51:1355–1364, 2011.
25. Inai Y and Nishikimi M. Increased degradation of oxidized proteins in yeast defective in 26 S proteasome assembly. *Arch Biochem Biophys* 404: 279–284, 2002.

26. Jung T, Catalgol B, and Grune T. The proteasomal system. *Mol Aspects Med* 30: 191–296, 2009.
27. Kirkin V, McEwan DG, Novak I, and Dikic I. A role for ubiquitin in selective autophagy. *Mol Cell* 34: 259–269, 2009.
28. Köhler A, Cascio P, Leggett DS, Woo KM, Goldberg AL, and Finley D. The axial channel of the proteasome core particle is gated by the Rpt2 ATPase and controls both substrate entry and product release. *Mol Cell* 7:1143–1152, 2001.
29. Kopp F, Hendil KB, Dahlmann B, Kristensen P, Sobek A, and Uerkvitz W. Subunit arrangement in the human 20S proteasome. *Proc Natl Acad Sci U S A* 94: 2939–2944, 1997.
30. Kriegenburg F, Poulsen EG, Koch A, Kruger E, and Hartmann-Petersen R. Redox control of the ubiquitin-proteasome system: from molecular mechanisms to functional significance. *Antiox Redox Signal* 15: 2265–2299, 2011.
31. Levine RL, Williams JA, Stadtman ER, and Shacter E. Carbonyl assays for determination of oxidatively modified proteins. *Methods Enzymol* 233: 346–357, 1994.
32. Lindersson E, Beedholm R, Hojrup P, Moos T, Gai W, Hendil KB, and Jensen PH. Proteasomal inhibition by alpha-synuclein filaments and oligomers. *J Biol Chem* 279: 12924–12934, 2004.
33. Liu CW, Corboy MJ, DeMartino GN, and Thomas PJ. Endoproteolytic activity of the proteasome. *Science* 299: 408–411, 2003.
34. Mieyal JJ, Gallogly MM, Qanungo S, Sabens EA, and Shelton MD. Molecular mechanisms and clinical implications of reversible protein S-glutathionylation. *Antioxid Redox Signal* 10: 1941–1988, 2008.
35. Niture SK, Velu CS, Bailey NI, and Srivenugopal KS. S-thiolation mimicry: quantitative and kinetic analysis of redox status of protein cysteines by glutathione-affinity chromatography. *Arch Biochem Biophys* 444: 174–184, 2005.
36. Osmulski PA and Gaczynska M. Atomic force microscopy reveals two conformations of the 20 S proteasome from fission yeast. *J Biol Chem* 275: 13171–13174, 2000.
37. Osmulski PA and Gaczynska M. Nanoenzymology of the 20S proteasome: proteasomal actions are controlled by the allosteric transition. *Biochemistry* 41: 7047–7053, 2002.
38. Osmulski PA, Hochstrasser M, and Gaczynska M. A tetrahedral transition state at the active sites of the 20S proteasome is coupled to opening of the alpha-ring channel. *Structure* 17: 1137–1147, 2009.
39. Pacifici RE, Kono Y, and Davies KJ. Hydrophobicity as the signal for selective degradation of hydroxyl radical-modified hemoglobin by the multicatalytic proteinase complex, proteasome. *J Biol Chem* 268: 15405–15411, 1993.
40. Peth A, Besche HC, and Goldberg AL. Ubiquitinated proteins activate the proteasome by binding to Usp14/Ubp6, which causes 20S gate opening. *Mol Cell* 36:794–804, 2009.
41. Rabl J, Smith DM, Yu Y, Chang SC, Goldberg AL, and Cheng Y. Mechanism of gate opening in the 20S proteasome by the proteasomal ATPases. *Mol Cell* 30: 360–368, 2008.
42. Religa TL, Sprangers R, and Kay LE. Dynamic regulation of archaeal proteasome gate opening as studied by TROSY NMR. *Science* 328: 98–102, 2010.
43. Rogers N, Paine S, Bedford L, and Layfield R. Review: the ubiquitin-proteasome system: contributions to cell death or survival in neurodegeneration. *Neuropathol Appl Neurobiol* 36: 113–124, 2010.
44. Shang F and Taylor A. Ubiquitin-proteasome pathway and cellular responses to oxidative stress. *Free Radic Biol Med* 51: 5–16, 2011.
45. Shringarpure R, Grune T, Mehlhase J, and Davies KJ. Ubiquitin conjugation is not required for the degradation of oxidized proteins by proteasome. *J Biol Chem* 278: 311–318, 2003.
46. Silva GM, Netto LE, Discola KF, Piassa-Filho GM, Pimenta DC, Barcena JA, and Demasi M. Role of glutaredoxin 2 and cytosolic thioredoxins in cysteinyl-based redox modification of the 20S proteasome. *FEBS J* 275: 2942–2955, 2008.
47. Smith DM, Chang SC, Park S, Finley D, Cheng Y, and Goldberg AL. Docking of the proteasomal ATPases' carboxyl termini in the 20S proteasome's alpha ring opens the gate for substrate entry. *Mol Cell* 27: 731–744, 2007.
48. Tanahashi N, Murakami Y, Minami Y, Shimbara N, Hendil KB, and Tanaka K. Hybrid proteasomes. Induction by interferon-gamma and contribution to ATP-dependent proteolysis. *J Biol Chem* 275: 14336–14345, 2000.
49. Tian G, Park S, Lee MJ, Huck B, McAllister F, Hill CP, Gygi SP, and Finley D. An asymmetric interface between the regulatory and core particles of the proteasome. *Nat Struct Mol Biol* 18: 1259–1267, 2011.
50. Tofaris GK, Layfield R, and Spillantini MG. alpha-synuclein metabolism and aggregation is linked to ubiquitin-independent degradation by the proteasome. *FEBS Lett* 509: 22–26, 2001.
51. Verma R, Chen S, Feldman R, Schieltz D, Yates J, Dohmen J, and Deshaies RJ. Proteasomal proteomics: identification of nucleotide-sensitive proteasome-interacting proteins by mass spectrometric analysis of affinity-purified proteasomes. *Mol Biol Cell* 11: 3425–3439, 2000.
52. Wang X, Yen J, Kaiser P, and Huang L. Regulation of the 26S proteasome complex during oxidative stress. *Sci Signal* 3: ra88–98, 2010.
53. Winterbourn CC and Hampton MB. Thiol chemistry and specificity in redox signaling. *Free Radic Biol Med* 45: 549–561, 2008.
54. Yang Y, Shi W, Chen X, Cui N, Konduru AS, Shi Y, Trower TC, Zhang S, and Jiang C. Molecular basis and structural insight of vascular K(ATP) channel gating by S-glutathionylation. *J Biol Chem* 286: 9298–9307, 2011.
55. Zhao X and Yang J. Amyloid-beta peptide is a substrate of the human 20S proteasome. *ACS Chem Neurosci* 1: 655–660, 2010.

Address correspondence to:
Dr. Marilene Demasi
Instituto Butantan
Laboratório de Bioquímica e Biofísica
Avenida Vital Brasil, 1500
São Paulo, SP, CEP: 05503-001
Brasil

E-mail: marimasi@butantan.gov.br

Dr. Luis E.S. Netto
Instituto de Biociencias
Universidade de São Paulo
Rua do Matao, 277
05508-090
Sao Paulo-SP
Brasil

E-mail: nettoles@ib.usp.br

Date of first submission to ARS Central, August 2, 2011; date of final revised submission, January 4, 2012; date of acceptance, January 4, 2012.

Abbreviations Used

2-DE = two-dimensional electrophoresis
3D = three-dimensional
20SPT = 20S catalytic unit of the proteasome
ΔNα3α7 20SPT = 20SPT purified from the SUB556 strain
BSA_{ox} = oxidized bovine serum albumin
ChT-L = chymotrypsin-like
Cys = cysteine
Cys-SOH = cysteine sulfenic acid
Cys-SO_2H = cysteine sulfinic acid
DNPH = dinitrophenylhydrazine
DTPA = diethylene triamine pentaacetic acid
DTT = dithiothreitol
FITC = fluorescein isothiocyanate
Grx2 = glutaredoxin 2
GSH = reduced glutathione
GSSG = oxidized glutathione
LC-MS/MS = liquid chromatography–tandem mass spectrometry
LC-Q-ToF-MS = liquid chromatography-quadrupole-time of flight-mass spectrometry
NBD = 7-chloro-4-nitrobenzo-2-oxa-1,3-diazole
nPT-SG = natively S-glutathiolated 20S proteasome purified from yeast grown in YPD medium to stationary phase
PAGE = polyacrylamide gel electrophoresis
PT-SH = DTT-reduced 20S proteasome
PT-SG = *in vitro* S-glutathiolated 20S proteasome
SAXS = small-angle X-ray scattering
SDS = sodium dodecyl sulfate
TEM = transmission electron microscopy
UPS = ubiquitin-proteasome system